Electrochemical Science Advances

WILEY-VCH

ELECTROCHEMICAL SCIENCE ADVANCES Open Access

RESEARCH ARTICLE OPEN ACCESS

Electrochemical Studies of Benzoquinone, Hydrobenzoquinone, Diphenoquinone and Hydrodiphenoquinone-Based Compounds

Flávia Leitão[1] | Daniel Galrito[1] | Luís C. Branco[1] | Hugo Cruz[1,2] | Paula S. Branco[1]

[1]Department of Chemistry, LAQV@REQUIMTE, Nova School of Science and Technology, Nova University of Lisbon, Caparica, Portugal | [2]INL–International Iberian Nanotechnology Laboratory, Avenida Mestre José Veiga, Braga, Portugal

Correspondence: Paula S. Branco (paula.branco@fct.unl.pt) | Hugo Cruz (hugo.cruz@inl.int)

Received: 4 October 2024 | **Revised:** 13 December 2024 | **Accepted:** 26 February 2025

Funding: This work received support and help from FCT/MCTES (LA/P/0008/2020 DOI 10.54499/LA/P/0008/2020, UIDP/50006/2020 DOI 10.54499/UIDP/50006/2020 and UIDB/50006/2020 DOI 10.54499/UIDB/50006/2020), through national funds and project PTDC/QUI-QOR/7450/2020 'Organic Redox Mediators For Energy Conversion' through Fundação para a Ciência e a Tecnologia I. P.-FCT. FCT/MCTES is also acknowledged for the National NMR Facility (RECI/BBB-BQB/0230/2012 and RECI/BBB-BEP/0124/2012).

Keywords: cyclic voltammetry | diphenoquinone | hydrobenzoquinone | hydrodiphenoquinone | quinones

ABSTRACT

Several quinones, diphenoquinones and respective reduced forms, hydrobenzoquinones and hydrodiphenoquinones, were synthesized, and their electrochemical properties were studied by cyclic voltammetry (CV) in non-aqueous medium to assess their upcoming applicability as organic redox mediators. Benzoquinones and diphenoquinones exhibited two reversible electron transfers (ETs) as exemplified by tetra-*tert*-butyldiphenoquinone, which displayed ETs at standard potential (E^0) at $E^0 = -0.53$ V and $E^0 = -0.92$ V versus SCE (saturated calomel electrode). However, hydrobenzoquinones displayed chemically irreversible ET, whereas hydrodiphenoquinones exhibited either chemically irreversible or quasi-reversible ETs. For instance, di-*tert*-butylhydrobenzoquinone demonstrated two irreversible ETs at $E_{pc} = 0.31$ V and $E_{pa} = 1.00$ V versus SCE.

1 | Introduction

Redox mediators are compounds, often in the form of neutral molecules or ions, that play a crucial role in facilitating electron transfer (ET) during electrochemical processes. These mediators act as intermediate electron carriers or reservoirs, capable of undergoing reversible oxidation and reduction reactions as they shuttle electrons between a substrate and an electrode. The incorporation of redox mediators enlarged the horizons of electrochemical synthesis with a pivotal role in the field of electrocatalysis and electrosynthesis [1]. Redox processes play a fundamental role in various electrochemical devices, including dye-sensitized solar cells (DSSCs) [2a, 2b], batteries [3a, 3b] and electrochromic cells [4]. The performance of these technologies depends on several critical factors, such as the reactivity of the redox mediators, the interface between electrodes and the electroactive species (substrates) and the overall configuration of the electrochemical cells. Some of these systems pose challenges such as high cost, toxicity, use of scarce metals and recyclability, among other issues. Organic redox mediators (ORMs), as the name suggests, are organic compounds that offer several advantages compared to their traditional inorganic counterparts. In addition, ORMs are often more stable than inorganic mediators, which can improve the longevity of energy conversion or storage systems [5]. In energy conversion and storage, inorganic materials, such as vanadium, iron and manganese, are commonly used as redox mediators in flow batteries, whereas lithium, cobalt and nickel serve as solid lithium intercalation materials in

conventional batteries. However, the extraction and processing of these materials are energy-intensive and can lead to significant environmental harm. In addition, inorganic materials are often non-renewable and, once mined, cannot be regenerated. ORMs are a promising alternative to the metal-based electrolytes for redox flow batteries (RFBs) due to the low-cost (compared with vanadium systems) and high-performance operation [1, 3a]. These advantages include affordability, widespread availability, biodegradability and the potential for production from renewable resources [6]. Quinones are among the principal and extensively studied organic redox couples, possessing a significant contribution to advancing our knowledge of organic redox chemistry from a foundational perspective [7]. The bulk of these studies took place in pH-buffered solutions, where the redox reaction of quinones is typically characterized as a two-electron, two-proton reduction to yield hydroquinone. In non-buffered water, the reduction proceeds by forming the highly hydrogen-bonded quinone dianion through a two-electron process. This dianion exists as an equilibrium mixture of protonation states in water [8]. Lehmann and Evans reported a peculiar behaviour of several benzoquinones in acetonitrile [9]. It is interesting to emphasize the observation that the cyclic voltammograms consistently revealed distinctive deviations from the expected patterns of sequential quinone reduction to its radical anion and dianion forms [9]. Quinones are widely prevalent in nature, and living organisms utilize them for their redox properties. Examples include ubiquinone, involved in the electron transport chain of oxidative phosphorylation, and plastoquinone, crucial for photosynthesis [10]. A more recent addition to this category is phoenicin, a fungal-derived quinone that is currently being explored for its potential utility in RFBs. In an aqueous RFB, phoenicin was employed as an anolyte alongside hexacyanoferrate(II), yielding an impressive open circuit voltage (OCV) of 0.87 V [11]. Quinones belong to a versatile class of organic compounds that can be easily tailored through chemical derivatization. Certain quinone-based redox mediators showed performance levels that approach those observed in vanadium-based RFBs [3a, 12a,b]. Huskinson et al. introduced a pioneering approach by employing 9,10-anthraquinone-2,7-disulfonic acid (AQDS) as an ORM in aqueous RFBs, specifically against bromine/bromide [13]. Their work achieved an impressive OCV of 0.8 V, demonstrating remarkable power density, marking a significant milestone in quinone application within RFB technology. The hydroquinone/quinone redox couple application in batteries for decoupled water splitting demonstrates their improved applicability and stability [14a,b] with a tetrasubstituted benzoquinone/hydrobenzoquinone pair found to be substantially more stable than AHQDS/AQDS [14b]. Diphenoquinones were not as studied as benzoquinones. Its core structure is present in several compounds with biological activity [15a,b] and was also studied using both electrochemical and computational tools for potential application in ORFB [16]. When compared to benzoquinones, diphenoquinones show higher reduction potentials, with unsubstituted diphenoquinones producing reduction potentials of −0.608 and −0.787 V versus Fc/Fc^+ [16]. The reduction products of benzoquinones and diphenoquinones are hydrobenzoquinones and hydrodiphenoquinones (or biphenols), respectively. Biphenols, specially 4,4′-biphenol, were used as a redox mediator for the determination of cysteine and glutathione by cyclic voltammetry (CV) with the results showing the catalytic current being dependent on the concentration of glutathione or *N*-acetylcysteine and solution's pH [17a,b]. The electrochemical oxidation of 4,4′-biphenol in the presence of 2-mercaptobenzimidazole was reported by Nematollahi and collaborators [18], allowing the synthesis of 2-(phenylthio)-1*H*-benzo[d]imidazole derivatives.

Benzoquinones are generally synthesized from substituted phenols through their oxidation. Several processes exist to perform this oxidation, such as reaction with lead dioxide and 70% $HClO_4$ in acetic acid [19] or by the use of oxygen in the presence of cobalt salen complexes or analogues [20] as well as using an oxidizer such as (diacetoxyiodo)benzene [21]. A more sustainable alternative appeals to the electrochemical oxidation in flow, avoiding the use of stoichiometric oxidizers or expensive catalysts [22]. As for the preparation of diphenoquinones, usually it requires the oxidation of either phenols or 4,4′-biphenols (or 4,4′-hydrodiphenoquinones). The synthesis of diphenoquinones has been previously reported in the presence of $Mn(OAc)_3$ while using $Mn(acac)_3$ instead produces the hydrodiphenoquinone [23]. Diphenoquinones have also been prepared by the oxidation of phenols. Hydrobenzoquinones and hydrodiphenoquinones are usually prepared via the reduction of benzoquinones and diphenoquinones, respectively. This reduction can be performed using common reduction procedures, such as hydrochloric acid and tin(II) chloride [24], hydrogen over Raney nickel [25], acetic acid with zinc dust [26] or with hydrogen over ruthenium [27].

Herein, several benzoquinones, diphenoquinones and respective reduced forms, hydrobenzoquinones and hydrodiphenoquinones, were synthesized, and their electrochemical properties were studied by cyclic voltammetry (CV) in order to understand their potential for future application as ORMs, namely in non-aqueous RFB.

2 | Results and Discussion

2.1 | Synthesis

In this work, benzoquinones (**1**) were synthesized by oxidation of 2,6-substituted phenols with (diacetoxyiodo)benzene following the procedure of Scheiber et al. [21], whereas diphenoquinones (**3**) were synthesized by oxidation with cerium ammonium nitrate (CAN) in the presence of $HClO_4$ (Scheme 1), following a procedure adapted from that of Domagała et al. [28]. The respective hydrobenzoquinones (**2**) and hydrodiphenoquinones (**4**) were produced by reduction of **1** and **3**, respectively, with zinc in acetic acid at 70°C (Scheme 1), following the procedure of Coffield et al. [26]. All the compounds were obtained in good to excellent yields. In terms of stability, diphenoquinones proved to be the most promising compounds when compared to benzoquinones, hydrobenzoquinones and hydrodiphenoquinones. However, all four families of compounds showed some degree of degradation. Both hydrobenzoquinones and hydrodiphenoquinones are very susceptible to re-oxidize to benzoquinones and diphenoquinones, respectively. Due to this, all these families of compounds were freshly purified before every cyclic voltammetry analysis.

2.2 | Cyclic Voltammetry (CV) Studies

Although there have been reported studies on the CV of specific quinones to address specific objectives, the same cannot be

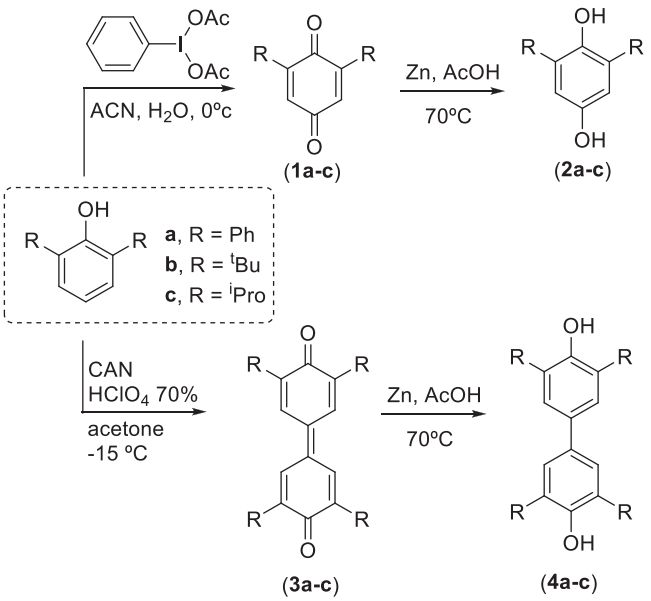

SCHEME 1 | Synthetic pathway for benzoquinones (**1**), diphenoquinones (**3**) and respective hydrobenzoquinones (**2**) and hydrodiphenoquinones (**4**).

said for diphenoquinones. Consequently, a systematic investigation of these compounds, including their reduced forms, and a comparative analysis between them is currently lacking. With the prospect of future applications in RFB, 12 compounds were selected according to their solubility in organic solvents, and an in-depth study of their electrochemical behaviour was conducted. CV studies were performed for all benzoquinones (**1**), diphenoquinones (**3**), hydrobenzoquinones (**2**) and hydrodiphenoquinones (**4**). In Table 1, the standard potential (potential for the reversible ETs) is presented for all studied compounds calculated as the average set by the cathodic and anodic peaks. The number of electrons associated with an ET was calculated by comparison to the standard ferrocene electrochemical probe in the same experimental conditions. The reversibility of ETs was calculated using the formula i_{pa}/i_{pc}, where i_{pa} is the anodic peak current and i_{pc} cathodic peak current.

2.2.1 | Diphenoquinones and Hydrodiphenoquinones

All diphenoquinones (**3a–c**) exhibited two successive, reversible and single-ET processes. The first corresponds to the reduction of the diphenoquinones forming a semiquinone radical anion, whereas the second reduction leads to the formation of the dianion (see Scheme 2, Table 1, Entries 7–11 and Figure S1, ESI). These species can be easily protonated in solution, and it is important to eliminate water from the selected organic solvents. Molecular sieves were employed both in the solution and in the bubbler to minimize any water that could potentially enter the cell during the electrochemical experiments.

In the absence of proton sources, the most likely reaction for the intermediates shown in Scheme 2 is the dimerization of two radical molecules (the isolation of potential dimerization products was not undertaken due to the structural diversity of possible products and the need for enough quantity for structural elucidation). Diphenoquinone **3a** exhibited several minor chemically irreversible ET processes. A possible explanation for these ETs may be linked to the compound's extended conjugation system, where parallel reactions can occur at reactive sites. These ETs were observed at standard potentials of $E^0 = -0.09$ V and $E^0 = -0.47$ V versus SCE (Table 1, Entry 7), respectively, for diphenoquinone **3a**.

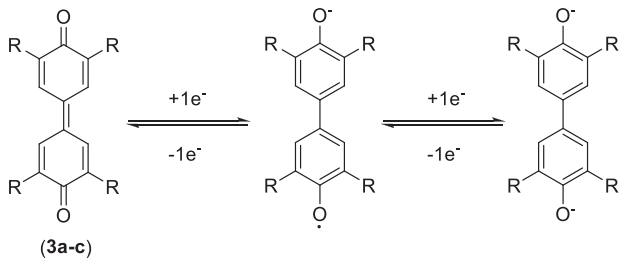

SCHEME 2 | The reduction process of the diphenoquinones (**3a–c**) (1 mM) to the dianion in DMF or MeCN solution in the presence of tetrabutylammonium hexafluorophosphate-[TBA]PF_6 (100 mM).

This behaviour aligns with the observations of Hapiot and Pinson [29] on the electrochemical oxidation of 2,6-diphenylphenolates in acetonitrile where a variety of mechanisms are operative. Their study demonstrated that 2,6-diphenylphenolate undergoes irreversibly oxidization via a radical–radical coupling reaction to form a dimer which is subsequently oxidized to diphenoquinone (**3a**). These observations are consistent with a rate-determining coupling of two phenoxyl radicals. In the reverse scan, they have observed two small reversible peaks visible at a more negative potential: −0.23 and −0.45 V versus SCE at the same potential as the reversible reduction of 4,4′-diphenoquinone. Tetra-*tert*-butyl diphenoquinone (**3b**) was studied in MeCN, as well as dimethylformamide (DMF). In both solvents, it exhibited two successive mono-electronic ETs that present a reversible mono-electronic ET at all studied scan rates, as illustrated in Figure 1. In MeCN, these ETs occurred at $E^0 = -0.53$ V and $E^0 = -0.92$ V versus SCE, whereas in DMF they occurred at $E^0 = -0.35$ V and $E^0 = -0.87$ V versus SCE (Table 1, Entries 8 and 9). Both ETs presented, in both solvents, an almost complete reversibility profile (approx. 100%). It is more difficult to form the radical anion and dianion in MeCN than in DMF, resulting in the shift to more negative potentials. A possible explanation for that difference in the potentials could be attributed to the difference in thermodynamic potentials between DMF and MeCN (the standard potential in MeCN solutions is lower than the ones observed for the DMF) [30]. This is consistent with our experimental data, as shown Table 1. According to the literature, the stability of the electrogenerated radical may depend on several factors, with one of the most relevant being the stability within the media in which it is formed. Solvent effects on the redox properties of radicals have been studied extensively. For example, Jonsson et al. [31a,b] focused on the first one-electron reduction of some *para*-quinones. The effect of solvents on redox potentials can serve as an indicator of the solvent's influence on the solvation of a redox couple. Thus, the redox potential is intensely influenced by the nature of the solvent. Solvent sensitivity rises with charge localization. In this way, it could be expected that the single-ET process could be strongly solvent-dependent due to solvent stabilization of the electrogenerated charged species. The authors

TABLE 1 | Potentials of the most significant electron transfers for all compounds studied.

Entry	Compound	Solvent[a]	Da ($\times 10^{-6}$)	Dc ($\times 10^{-6}$)	I_{pa}/I_{pc}[b]	Potential (V vs. SCE)							
						$E^0{}_1$[c]	$E^0{}_2$[c]	E_{pa1}[d]	E_{pc1}[d]	ΔE_{p1}	E_{pa2}[d]	E_{pc2}[d]	ΔE_{p2}
1	**1a**	MeCN	1.28	1.54	0.9	−0.47	—	−0.43	−0.50	0.07	—	−1.19	—
2	**1b**	MeCN	1.54	1.54	1	−0.69	—	−0.65	−0.73	0.08	—	−1.50	—
3	**1c**	MeCN	1.54	1.54	1	−0.67	—	−0.63	−0.71	0.08	—	−1.39	—
4	**2a**	MeCN				—	—	0.76	0.34	—	1.04	0.65	—
5	**2b**	MeCN			—	—	—	1.00	—	—	—	—	—
6	**2c**	MeCN				—	—	1.00	0.63	—	1.84	0.88	—
7	**3a**	DMF	0.71	0.71	0.8	−0.09	−0.47	−0.06	−0.13	0.07	−0.43	−0.51	0.08
8	**3b**	MeCN	0.71	1.31	0.9	−0.53	−0.92	−0.49	−0.56	0.07	−0.88	−0.96	0.08
9		DMF			0.9	−0.35	−0.87	−0.31	−0.39	0.08	−0.81	−0.92	0.11
10	**3c**	MeCN	0.71	1.03	0.8	−0.46	−0.81	−0.42	−0.50	0.08	−0.76	−0.85	0.09
11		DMF			0.9	−0.32	−0.75	−0.28	−0.35	0.07	−0.70	−0.79	0.09
12	**4a**	MeCN			0.5	—	—	0.98	0.73	—	1.13	0.99	—
13		DMF			—	—	—	0.78	0.32	—	—	—	—
14	**4b**	MeCN			—	—	—	1.06	0.64	—	—	—	—
15	**4c**	MeCN			—	—	—	1.05	0.75	—	—	—	—

Note: These potentials were measured at a scan rate of 0.10 V/s.

Abbreviation: SCE, saturated calomel electrode.

[a]MeCN (acetonitrile); DMF (dimethylformamide).

[b]Peak current intensity I_{pa} (a) anodic and I_{pc} (c) cathodic.

[c]E^0 standard potential E_1^0 standard potential first electron transfer and E_2^0 standard potential second electron transfer.

[d]E_p Peak Potential E_{pa} anodic peak potential and E_{pc} cathodic peak potential.

describe in this work that in the presence of a series of solvents, the reduction potentials of radicals increase from MeCN to DMF, with a trend as E^0 MeCN < E^0 DMF [30]. The half-wave potential, defined as the potential at which the current intensity reaches half of the peak current for oxidation or reduction, is equivalent to the standard potential for fast kinetics. It can be calculated by $E^0 = 0.5 \times (E_{Pa} + E_{Pc})$. But, for slow kinetics, these results are not the same because they are affected by alpha (α) constant obtained from the Butler–Volmer equation that describes the relationship between the current density (J) and the electrode potential (E) during an electrochemical reaction. Now the equation considers the kinetics of the redox process and incorporates the exchange current density (J_0) and the transfer coefficient (α) as follows:

$$J = J_0[\exp(\alpha\ n\ F\ (E - E^0)\ /\mathrm{RT}) - \exp(-(1-\alpha)nF\ (E - E^0)\ /\mathrm{RT})]$$

where E^0 is the standard potential.

Moreover, from the Randles–Sevcik equation-based analysis, the redox process can be considered reversible if peak current function ($I_p/v^{1/2}$) is independent of the scan rate, where the peak current is given by the Randles–Sevcik equation as presented in Figures S39 and S40 (ESI). Peak current intensity ratio (I_{pa}/I_{pc}) is 1 for all scan rates evaluated by the Randles–Sevcik equation, and peak potential separation ΔE_p at all scan rates is ~59/n mV. As can be observed in Table 1, the ratio I_{pa}/I_{pc} is 1 for just two examples, compounds **1b** and **1c** (Entry 2 and 3, Table 1), and ranges from 0.9 to 0.8 for the other family of compounds **2** and **3**, which leads to two reversible and a quasi-reversible process, respectively, in accordance to the Randles–Sevcik equation. Another important parameter to take in consideration for understanding the reversibility is the peak separation for all studied cases, which is higher than 59 mV/n. In one-ET reaction, the theoretical peak-to-peak separation is 59 mV at room temperature (25°C). In our case, kinetic parameters at the electrode surface may influence the peak-to-peak separation, and there may also be some IR drop that was not fully compensated.

In Table 1, Columns 4 and 5 are presented with the diffusion coefficients, and Column 6 is the I_{pa}/I_{pc}. These compounds are highly sensitive to oxygen and moisture in solution which can partially regulate the rate of ET process. As a result, they exhibit quasi-reversible behaviour over the time scale of our scans. The diffusion coefficients of the redox family of compounds **1** and **3** were calculated by the Randles–Sevcik equation and are presented in Table 1. It can be observed that for compounds **1a–c,** the formation of the radical cation presents a slightly higher diffusion coefficient than the reverting to the neutral species. For the compounds **3b–c**, the behaviour is in the other way; the re-oxidation of the radical diffuses faster than the neutral species. Of all the studied diphenoquinones, **3b** presented the lowest potentials; as such, it would be the most fit as an anolyte in ORFBs, leading to increased cell voltages.

This compound has also been studied previously by Néron et al. [16], observing a behaviour similar to that reported here. Néron

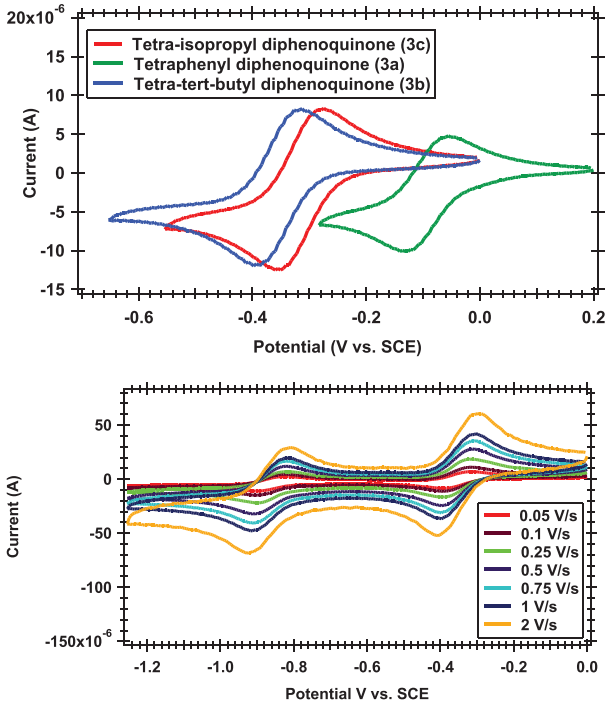

FIGURE 1 | On the top, the voltammograms of the three benzoquinones start from 0.2 or 0 to −0.2, −0.5 or −0.7 and return to 0.2 or 0 depending on the compound (**3a**–**c**) in MeCN, and on the bottom, the voltammograms of tetra-*tert*-butyl diphenoquinone (**3b**) in MeCN, at different scan rates, start from 0 to −1.2 and return to 0; the potentials are presented in V versus SCE. SCE, saturated calomel electrode.

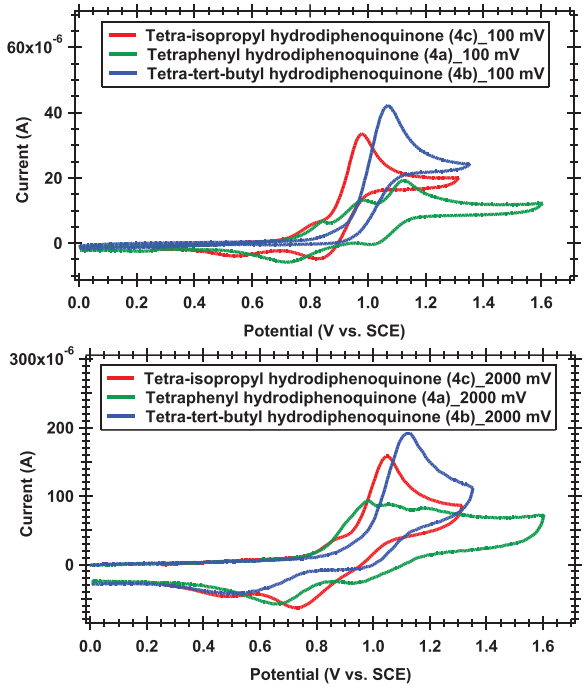

FIGURE 2 | Voltammograms of the three hydrodiphenoquinones starting from 0 to 1.2, 1.3 or 1.6 and returning to 0 (**4a**–**c**) in MeCN, at a scan rate of 0.10 V/s (top) and 2 V/s (bottom), the potentials are presented in V versus SCE. SCE, saturated calomel electrode.

et al. studied the electrochemical properties of **3b** in MeCN, using tetrabutylammonium hexafluorophosphate as supporting electrolyte, at multiple scan rates in the range of 0.10–5 V/s. They identified two successive reversible mono-electronic ETs corresponding by the formation of the semiquinone radical anion, followed by formation of the dianion, as we have observed in our case (Figure 1). The first transfer was observed at $E^0 = -0.503$ V and the second at $E^0 = -0.808$ V versus SCE. Tetraisopropyl diphenoquinone (**3c**) was also studied in both MeCN and DMF (Table 1, Entries 10 and 11). In both solvents, two successive mono-electronic ETs were presented, being reversible; the radical anion and dianion formed are stable in both electrolytes at all studied scan rates. In MeCN, the ETs occur at $E^0 = -0.46$ V and $E^0 = -0.81$ V versus SCE, whereas in DMF, they occur at $E^0 = -0.32$ V and $E^0 = -0.75$ V versus SCE, following the same trend observed for the tetra-*tert*-butyl diphenoquinone (**3b**). It is more difficult to form the radical anion in MeCN. The observed reversibility in diphenoquinones (**3a**–**c**) can be attributed to the oxidation/reduction process depicted in Figure 1. In all scan rates, the three diphenoquinones presented two successive reversible mono-electronic ETs. Of these compounds, the tetra-*tert*-butyl diphenoquinone (**3b**) presented ETs at lowest potentials of all the studied diphenoquinones.

From the literature, in the case of 4,4-biphenol/4,4-diphenoquinone (compounds not studied by us), the reversibility enabled its application as a redox mediator by facilitating the homogeneous electrocatalysis of glutathione, *N*-acetylcysteine [17b] and cysteine [17a] in aqueous medium. In our study, fully reversible two successive ETs are observed in organic solvents. But when in aqueous medium, these compounds could present one bi-electronic simultaneous ET or a chemically irreversible ET.

This does not imply that the reversibility obtained in organic solvents can be directly extrapolated to aqueous medium, as this family of compounds exhibits different behaviours in organic versus aqueous environments. The hydrodiphenoquinones (**4a**–**c**) presented either a chemical irreversible or quasi-reversible mono-electronic ET (Table 1, Entries 12 to 15) (Figure 2). The irreversibility is associated to a chemical reaction involving the species formed during the oxidation step. A possible explanation is the loss of an electron, resulting in the formation of a radical cation, which then undergoes deprotonation to form a radical that reacts further. As the potential shifts to more negative values, the species being reduced differs from the one generated during oxidation, causing the cathodic peak to shift further away from the anodic peak.

Tetraphenyl hydrodiphenoquinone (**4a**), in MeCN, displayed multiple ETs (Figure 3). At scan rates of 0.250 V/s and lower, it displayed three anodic peaks, the first of which disappears at higher scan rates, possibly by the overlapping of the second and third anodic peaks. These three ETs, the first appearing as a shoulder at $E_{pa} = 0.87$ V, the second a peak at $E_{pa} = 0.98$ V and the third also a peak at $E_{pa} = 1.13$ V versus SCE (Table 1, Entry 12), show a slight shift to higher potentials as the scan rate increases. It was also observed two cathodic peaks, approximately at $E_{pc} = 0.73$ V and $E_{pc} = 0.99$ V versus SCE. In DMF, however, it was observed only one anodic peak at $E_{pa} = 0.78$ V and one cathodic peak at $E_{pc} = 0.32$ V versus SCE (Table 1, Entry 13).

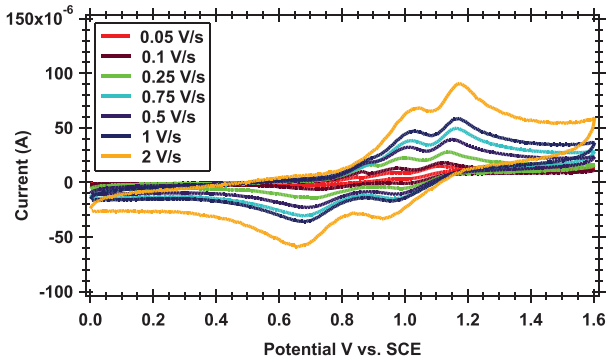

FIGURE 3 | Voltammograms of tetraphenyl hydrodiphenoquinone starting from 0 to 1.6 and returning to 0 (**4a**) in MeCN, at multiple scan rates, the potentials are presented in V versus SCE. SCE, saturated calomel electrode.

Tetra-*tert*-butylhydrodiphenoquinone (**4b**) presented a chemical irreversible ET, with an anodic peak at E_{pa} = 1.06 V versus SCE and a cathodic peak E_{pc} = 0.64 V versus SCE (Table 1, Entry 14). This cathodic ET is absent at scan rates lower than 0.250 V/s and steadily becomes bigger at higher scan rates. Tetraisopropyl diphenoquinone (**4c**) displayed an ET with quasi-reversible behaviour. An anodic peak occurs at E_{pa} = 1.05 V versus SCE and a cathodic peak at E_{pc} = 0.75 V versus SCE (Table 1, Entry 15). None of the three hydrodiphenoquinones presented fully reversible ETs; however, compound **4a** was the closest (Figure 3).

In this context, diphenoquinone **3b** appears to be the most suitable candidate for use as an anolyte. Among the hydrodiphenoquinones, compound **4a** demonstrated the highest standard potentials and the greatest reversibility, making it a potentially interesting option for use as a catholyte in RFBs.

2.2.2 | Benzoquinones and Hydrobenzoquinones

The three studied benzoquinones (**1**) exhibited similar behaviour (Figure 4), with a first reversible mono-electronic ET, similar to the first ET of diphenoquinones (**3a**–**c**). As for the second ET, multiple phenomena may overlap at the anodic peak because it presents either broad or sharp peaks depending on the conditions. This could be explained by chemical transformations or adsorption to the electrode surface. The most plausible explanation is that the re-oxidation of the dianion to the radical anion involves adsorption to the electrode surface, leading to the narrow, high-intensity peak observed during the re-oxidation process.

All benzoquinones' derivatives showed this behaviour; therefore, it is not possible to determine the reversibility of this ET. Comparing the first ET of benzoquinones **1b** and **1c** with diphenoquinones **3b** and **3c**, the last presented a slightly higher reduction potential. Benzoquinone **1a** exhibited three main ETs: The first is a mono-electronic reversible ET at E^0 = −0.47 V versus SCE (Table 1, Entry 1), followed by a chemical irreversible ET with an anodic peak at E_{pa} = −0.43 V versus SCE, and as described earlier, a sharp peak is observed at E_{pa} = −0.65 V versus SCE. The study of this benzoquinone also revealed a cathodic peak at E_{pc} = −1.19 V versus SCE.

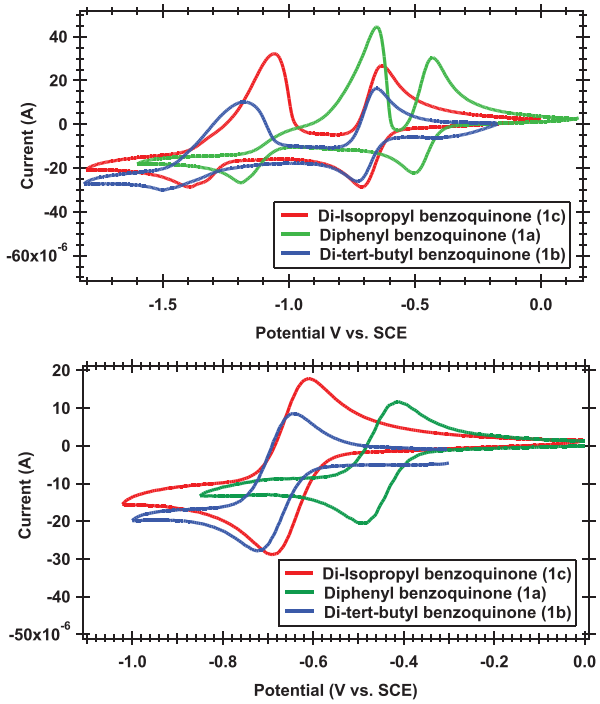

FIGURE 4 | Voltammograms of the three benzoquinones starting from 0 or −0.2 to −1.6 returning to 0 or −0.2 (**1a**–**c**) in MeCN, for two ET (top) and first ET (bottom) at a scan rate of 0.10 V/s, the potentials are presented in V versus SCE. SCE, saturated calomel electrode.

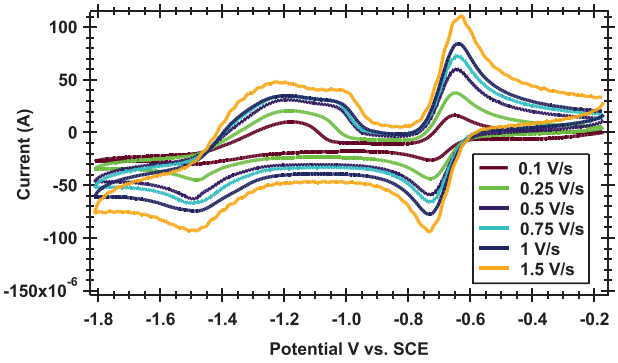

FIGURE 5 | Voltammogram of di-*tert*-butyl benzoquinone starting from 0 to −1.8 returning to 0 (**1b**) in MeCN, at different scan rates, the potentials are presented in V versus SCE. SCE, saturated calomel electrode.

The electrochemical reduction of 2,6-di-*tert*-butyl-1,4-benzoquinone (**1b**) has been previously studied in MeCN [9], and the obtained results are in agreement with the previously reported results for the first ET. Benzoquinone **1b** exhibited two major ETs (Figure 5). The first is a reversible mono-electronic ET at E^0 = −0.69 V versus SCE (Table 1, Entry 2). The second ET showed a broad anodic peak, making it challenging to accurately assess its reversibility under these experimental conditions. The cathodic peak of the second ET is observed at E_{pa} = −1.50 V versus SCE, which agrees with the study reported by Evans et al. [9]. The electrochemical study of benzoquinone **1c** showed a first mono-electronic ET at E^0 = −0.67 V versus SCE (Table 1, Entry 3), as described for the previous compound at E_{pa} = −0.87 V and

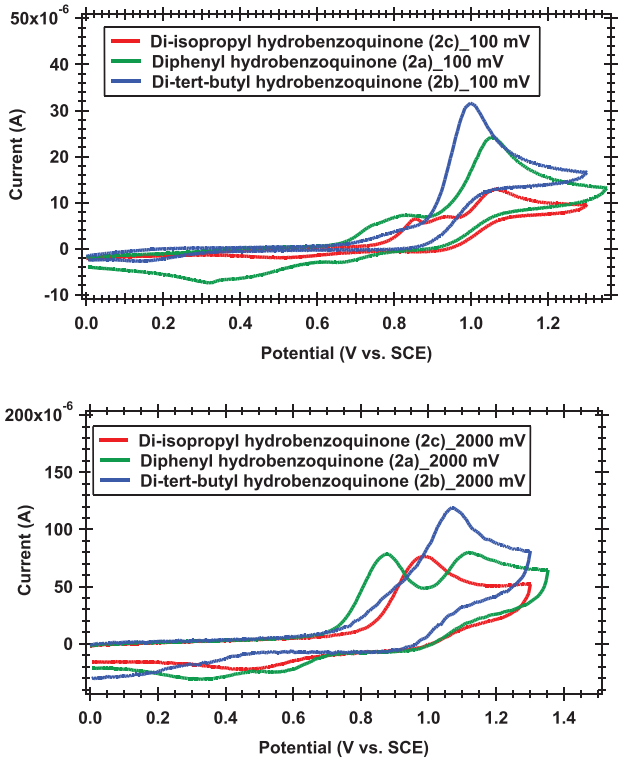

FIGURE 6 | Voltammograms of the three hydrobenzoquinones starting from 0 to 1.3 and returning to 0 (**2a–c**) in MeCN, at a scan rate of 0.10 V/s (top) and 2 V/s (bottom), the potentials are presented in V versus SCE. SCE, saturated calomel electrode.

E_{pa} = −1.19 V versus SCE and a cathodic peak at E_{pc} = −1.39 V versus SCE.

As for the hydrobenzoquinones (**2a–c**), they behaved similarly to the hydrodiphenoquinones (Figure 6), presenting chemically irreversible mono-electronic ETs (Table 1, Entries 4–6). As previously explained for the hydrodiphenoquinone family (**4a–c**), a potential explanation for the irreversibility observed in the hydrobenzoquinones (**2a–c**) is a chemical reaction occurring during the second ET. Various phenomena may overlap at the anodic peak, which can appear broader or sharper depending on the situation. These variations could be due to electrochemical and chemical transformations or adsorption to the electrode surface. Parallel reactions, such as dimerization between reduced and oxidized species, may also be occurring. Additionally, while less predictable, reactions with the solvent (such as protonation) cannot be entirely ruled out, despite the solvent being dried and purged with argon prior to the experiments.

Diphenyl hydrobenzoquinone (**2a**) presented two main chemical irreversible ETs (Figure S2, ESI). The first anodic peak appears at E_{pa} = 0.76 V versus SCE, at scan rates lower than 0.500 V/s. The second anodic peak is presented at approximately E_{pa} = 1.04 V versus SCE. Two cathodic peaks are also observed; the first is located at E_{pc} = 0.34 V and the second at E_{pc} = 0.65 V versus SCE (the second one appearing only at scan rates equal or higher than 0.500 V/s; Table 1, Entry 4).

The di-*tert*-butyl hydrobenzoquinone (**2b**) presented only one chemical irreversible ET, with an anodic peak E_{pa} = 1.00 V versus SCE and a small cathodic peak E_{pc} = 0.34 V versus SCE (Table 1, Entry 5). The di-isopropyl hydrobenzoquinone (**2c**) showed two chemical irreversible ETs, displaying two anodic peaks at E_{pa} = 1.00 V and E_{pa} = 1.84 V versus SCE and two cathodic peaks at E_{pc} = 0.63 V and E_{pc} = 0.88 V versus SCE (Table 1, Entry 6). The anodic peak at 1.84 V versus SCE appears to be unique among the studied hydrobenzoquinones; however, it is similar to that presented by the diphenoquinones and hydrodiphenoquinones. No hydrobenzoquinone stands out, as the three present an irreversible ET at E_{pa} ~1.00 V versus SCE, with compound **2c** possessing an ET at E_{pa} = 1.84 V versus SCE as well, although it is completely irreversible.

3 | Experimental Procedures

All reagents and solvents were obtained commercially from TCI, Sigma-Aldrich, Scharlau and Honeywell without further purification. When dry solvents were required, these were dried following a procedure described in the literature [32]. Nuclear magnetic resonance (NMR) spectra were acquired by a Bruker Avance III 400 spectrometer; ^{1}H and ^{13}C NMR spectra were measured at frequencies 400 and 101 MHz, respectively. Cyclic voltammetry (CV) was performed using an Autolab PGSTAT12 potentiostat/galvanostat electrochemical system, and the data were collected using the software GPES Manager 4.9. The measurements were made in a glass cylinder electrochemical cell, and the working electrode (WE) used was a glassy carbon electrode with a diameter of 3 mm, the counter-electrode (CE) used was a platinum wire, and the reference electrode (RE) was a saturated calomel electrode. The samples were prepared by dissolving the compound (1 mM) and supporting electrolyte (100 mM) in previously dried solvents (MeCN or DMF) in 3 Å molecular sieves. The solution was then degassed with argon for 20 min. CV measurements were done at multiple scan rates. Between each measurement, the WE was washed with ethanol and polished in 1.0 and 0.3 mm alumina polishing and washed again, whereas the solution was kept being degassed with argon in the downtime.

3.1 | Synthetic Methodology

3.1.1 | Synthesis of benzoquinones (1a–c)

Following a procedure described by Presser et al. [21], in a round flask bottom, the respective phenol was dissolved in acetonitrile (6.5 mL/mmol), water was added (2 mL/mmol), and the oxidizer, diacetoxyiodo(benzene) (DIB) (1.3 eq.), was slowly added at 0°C. The reaction was kept at 0°C until completion. Upon completion, the mixture was allowed to reach RT and then diluted with water and extracted with methylene chloride. The organic phase was dried with anhydrous Na_2SO_4 and evaporated to dryness under reduced pressure. Compounds were purified by flash chromatography using different mixtures of petroleum ether and methylene chloride.

2,6-Diphenyl-1,4-benzoquinone (**1a**): Following the general procedure, compound **1a** was obtained in 86% from 2,6-diphenylphenol (100 mg, 0.41 mmol) after 1 h of reaction. The mixture was purified by flash chromatography, using as

eluent a mixture of 6:4 (petroleum ether:methylene chloride). Spectroscopic data were in accordance with literature [33].

2,6-*Tert*-butyl-1,4-benzoquinone (**1b**): Following the general procedure, compound **1b** was obtained in 62% from 2,6-di-*tert*-butylphenol (100 mg, 0.48 mmol) after 2 h of reaction. The mixture was purified by flash chromatography, using as eluent a mixture of 9:1 (petroleum ether:methylene chloride). Spectroscopic data were in accordance with literature [34].

2,6-Isopropyl-1,4-benzoquinone (**1c**): Following the general procedure, compound **1c** was obtained in 83% from 2,6-diisopropylphenol (100 mg, 0.56 mmol) after 1 h of reaction. The mixture was purified by flash chromatography, using as eluent a mixture of 7:3 (petroleum ether:methylene chloride). Spectroscopic data were in accordance with literature [35].

3.1.2 | Synthesis of Hydrobenzoquinones and Hydrodiphenoquinones (2a–c and 4a–c)

Following the procedure described by Kolka et al. [26] in a round bottom flask, the respective benzoquinones (**1a**–**c**) or diphenoquinones (**3a**–**c**) were dissolved in acetic acid (5 mL/mmol), and zinc dust (5 eq. for hydrobenzoquinones and 7 eq. for hydrodiphenoquinones) was added to the mixture. The reaction was stirred at 70°C until the solution turned colourless. Upon completion, the mixture was left to reach room temperature and was poured over cold water. It was then extracted several times with ethyl acetate, and the organic phase was dried with anhydrous Na_2SO_4 and evaporated under reduced pressure.

2,6-Diphenyl-1,4-hydrobenzoquinone (**2a**): Following the general procedure, compound **2a** was obtained in 89% from 2,6-diphenyl-1,4-benzoquinone (**1a**) (84 mg, 0.32 mmol). Spectroscopic data were in accordance with literature [36].

2,6-Di-*tert*-butyl-1,4-hydrobenzoquinone (**2b**): Following the general procedure, compound **2b** was obtained in 92% from 2,6-di-tert-butyl-1,4-benzoquinone (**1b**) (69 mg, 0.31 mmol). Spectroscopic data were in accordance with literature [37].

2,6-Di-isopropyl-1,4-hydrobenzoquinone (**2c**): Following the general procedure, compound **2c** was obtained in 99% from 2,6-diisopropyl-1,4-benzoquinone (**1c**) (62 mg, 0.31 mmol). Spectroscopic data were in accordance with literature [38].

3,3′,5,5′-Tetraphenyl-4,4′-hydrodiphenoquinone (**4a**): Following the general procedure, compound **4a** was obtained in 85% from 3,3′,5,5′-tetraphenyl-4,4′-diphenoquinone (**3a**) (55 mg, 0.11 mmol). Spectroscopic data were in accordance with literature [39].

3,3′,5,5′-Tetra-*tert*-butyl-4,4′-hydrodiphenoquinone (**4b**): Following the general procedure, compound **4b** was obtained in 97% from 3,3′,5,5′-tetra-*tert*-butyl-4,4′-diphenoquinone (**3b**) (75 mg, 0.18 mmol). Spectroscopic data were in accordance with literature [39].

3,3′,5,5′-Tetraisopropyl-4,4′-hydrodiphenoquinone (**4c**): Following the general procedure, compound **4c** was obtained in 98% from 3,3′,5,5′-tetraisopropyl-4,4′-diphenoquinone (**3c**) (133 mg, 0.38 mmol). Spectroscopic data were in accordance with literature [40].

3.1.3 | Synthesis of Diphenoquinones (3a–c)

Following a procedure described by Kurosawa et al. [23] to a round bottom flask placed at −15°C, acetone (14.3 mL/mmol) was added, followed by perchloric acid (70%) (8 eq.), CAN (2.5 eq.) and finally the corresponding phenol. The mixture was allowed to stir at −15°C for 1 h, and upon completion, the mixture was diluted with water, the acetone was evaporated under reduced pressure, and the mixture was extracted with methylene chloride. The organic phase was dried with anhydrous Na_2SO_4 and evaporated under reduced pressure. The mixture was purified by flash chromatography using a mixture of solvents, petroleum ether and methylene chloride.

3,3′,5,5′-Tetraphenyl-4,4′-diphenoquinone (**3a**): Following the general procedure, compound **3a** was obtained in 64% from 2,6-diphenylphenol (100 mg, 0.41 mmol). The mixture was purified by flash chromatography, using as eluent a mixture of 6:4 (petroleum ether:methylene chloride).

3,3′,5,5′-Tetra-*tert*-butyl-4,4′-diphenoquinone (**3b**): Following the general procedure, compound **3b** was obtained in 91% from 2,6-di-tert-butylphenol (100 mg, 0.49 mmol). The mixture was purified by flash chromatography, using as eluent a mixture of 9:1 (petroleum ether:methylene chloride). Spectroscopic data were in accordance with literature [41].

3,3′,5,5′-Tetra-isopropyl-4,4′-diphenoquinone (**3c**): Following the general procedure, compound **3c** was obtained in 87% from 2,6-di-isopropylphenol (100 mg, 0.41 mmol). The mixture was purified by flash chromatography, using as eluent a mixture of 8:2 (petroleum ether:methylene chloride). Spectroscopic data were in accordance with literature [41].

3.1.4 | Cyclic Voltammetry (CV) Studies

CV studies were performed for all benzoquinones (**1**), hydrobenzoquinones (**2**), diphenoquinones (**3**) and hydrodiphenoquinones (**4**). The measurements were made in a 3-electrode cylindrical electrochemical cell, using a 3 mm glassy carbon electrode as the WE, a platinum wire as CE and a saturated calomel electrode as RE. All compounds were studied in a solution of tetrabutylammonium hexafluorophosphate in 100 mM concentration as the supporting electrolyte and the respective compound in 1 mM concentration. Due to the low solubility of diphenoquinone **3a** in acetonitrile, all three diphenoquinones (**3a**–**c**) were studied in DMF, as well as hydrodiphenoquinone **4a**. Benzoquinones (**1a**–**c**), hydrobenzoquinones (**2a**–**c**) and hydrodiphenoquinones **4b** and **4c** were studied in acetonitrile.

4 | Conclusion

This work was focused on the development of several quinones, diphenoquinones and their corresponding reduced forms,

hydrobenzoquinones and hydrodiphenoquinones. The tetra-*tert*-butyldiphenoquinone exhibited two reversible ETs, which displayed ETs at standard potential (E^0) at $E^0 = -0.53$ V and $E^0 = -0.92$ V versus SCE, a good example for the benzoquinones and diphenoquinones. However, for all the others, they displayed chemically irreversible ET, or either chemically irreversible or quasi-reversible ETs (as can be seen for the di-*tert*-butylhydrobenzoquinone that demonstrated two irreversible ETs at $E_{pc} = 0.31$ V and $E_{pa} = 1.00$ V versus SCE). These compounds are extremely sensitive to oxygen and moisture in solution that can regulate a part of the rate of ET process, leading then to become a quasi-reversible process on the time scale of our scan. Due to their wide range of redox potentials, quinones and hydroquinones have found applications in the field of energy storage, particularly in RFBs. One significant advantage of the developed compounds is the two-ET characteristic, which enhances the usefulness of quinones in the construction of all-quinone flow battery systems. From the gathered data in this study, diphenoquinones (**3**) seem to be the most promising family of compounds to apply in the RFBs.

Acknowledgements

This work received support and help from FCT/MCTES (LA/P/0008/2020 DOI 10.54499/LA/P/0008/2020, UIDP/50006/2020 DOI 10.54499/UIDP/50006/2020 and UIDB/50006/2020 DOI 10.54499/UIDB/50006/2020), through national funds and project PTDC/QUI-QOR/7450/2020 'Organic Redox Mediators For Energy Conversion' through Fundação para a Ciência e a Tecnologia I. P.-FCT. FCT/MCTES is also acknowledged for the National NMR Facility (RECI/BBB-BQB/0230/2012 and RECI/BBB-BEP/0124/2012).

Conflicts of Interest

The authors declare no conflicts of interest.

Data Availability Statement

Data are available in the article Supporting Information.

References

1. W. D. Shao, B. Lu, J. P. Cao, et al., "The Use of Redox Mediators in Electrocatalysis and Electrosynthesis," *Chemistry—An Asian Journal* 18 (2023): e202201093.

2. (a) M. Dhonde, K. Sahu, M. Das, A. Yadav, P. Ghosh, and V. V. S. Murty, "Review—Recent Advancements in Dye-Sensitized Solar Cells; From Photoelectrode to Counter Electrode," *Journal of the Electrochemical Society* 169 (2022): 066507. (b) F. Grifoni, M. Bonomo, W. Naim, et al., "Toward Sustainable, Colorless, and Transparent Photovoltaics: State of the Art and Perspectives for the Development of Selective Near-Infrared Dye-Sensitized Solar Cells," *Advanced Energy Materials* 11 (2021): 2101598.

3. (a) K. Wedege, D. Bae, W. A. Smith, A. Mendes, and A. Bentien, "Solar Redox Flow Batteries With Organic Redox Couples in Aqueous Electrolytes: A Minireview," *Journal of Physical Chemistry C* 122 (2018): 25729–25740. (b) A. Ramar, F. M. Wang, R. Foeng, and R. C. Hsing, "Organic Redox Flow Battery: Are Organic Redox Materials Suited to Aqueous Solvents or Organic Solvents?," *Journal of Power Sources* 558 (2023): 232611.

4. N. Jordao, H. Cruz, F. Pina, and L. C. Branco, "Studies of Bipyridinium Ionic Liquids and Deep Eutectic Solvents as Electrolytes for Electrochromic Devices," *Electrochimica Acta* 283 (2018): 718–726.

5. J. M. Cameron, C. Holc, A. J. Kibler, et al., "Molecular Redox Species for Next-Generation Batteries," *Chemical Society Reviews* 50 (2021): 5863–5883.

6. G. Kwon, Y. Ko, Y. Kim, K. Kim, and K. Kang, "Versatile Redox-Active Organic Materials for Rechargeable Energy Storage," *Accounts of Chemical Research* 54 (2021): 4423–4433.

7. J. Q. Chambers, "Electrochemistry of Quinones," in *The Quinonoid Compounds*, (John Wiley & Sons, Inc., 1988), 719–757.

8. M. Quan, D. Sanchez, M. F. Wasylkiw, and D. K. Smith, "Voltammetry of Quinones in Unbuffered Aqueous Solution: Reassessing the Roles of Proton Transfer and Hydrogen Bonding in the Aqueous Electrochemistry of Quinones," *Journal of the American Chemical Society* 129 (2007): 12847–12856.

9. M. W. Lehmann and D. H. Evans, "Anomalous Behavior in the Two-Step Reduction of Quinones in Acetonitrile," *Journal of Electroanalytical Chemistry* 500 (2001): 12–20.

10. H. Nohl, W. Jordan, and R. J. Youngman, "Quinones in Biology: Functions in Electron Transfer and Oxygen Activation," *Advances in Free Radical Biology and Medicine* 2 (1986): 211–279.

11. C. O. Wilhelmsen, S. B. Kristensen, O. Nolte, et al. *Batteries Supercaps* (2023): e202200365.

12. (a) J. B. Gerken, C. W. Anson, Y. Preger, et al., "Comparison of Quinone-Based Catholytes for Aqueous Redox Flow Batteries and Demonstration of Long-Term Stability With Tetrasubstituted Quinones," *Advanced Energy Materials* 10 (2020): 2000340. (b) Y. Preger, M. R. Johnson, S. Biswas, C. W. Anson, T. W. Root, and S. S. Stahl, "Anthraquinone-Mediated Fuel Cell Anode With an Off-Electrode Heterogeneous Catalyst Accessing High Power Density When Paired With a Mediated Cathode," *ACS Energy Letters* 5 (2020): 1407–1412.

13. B. Huskinson, M. P. Marshak, C. Suh, et al., "A Metal-Free Organic–Inorganic Aqueous Flow Battery," *Nature* 505 (2014): 195–198.

14. (a) B. Rausch, M. D. Symes, and L. Cronin, "A Bio-Inspired, Small Molecule Electron-Coupled-Proton Buffer for Decoupling the Half-Reactions of Electrolytic Water Splitting," *Journal of the American Chemical Society* 135 (2013): 13656–13659. (b) F. Wang, H. Y. Sheng, W. J. Li, J. B. Gerken, S. Jin, and S. S. Stahl, "Stable Tetrasubstituted Quinone Redox Reservoir for Enhancing Decoupled Hydrogen and Oxygen Evolution," *ACS Energy Letters* 6 (2021): 1533–1539.

15. (a) R. L. Edwards and H. J. Lockett, "Constituents of the Higher Fungi. Part XVI. Bulgarhodin and Bulgarein, Novel Benzofluoranthenequinones From the Fungus *Bulgaria inquinans*(Fries)," *Journal of the Chemical Society, Perkin Transactions* 1 (1976): 2149–2155. (b) J. J. Vollmer and J. Rosenson, "Chemistry of St. John's Wort: Hypericin and Hyperforin," *Journal of Chemical Education* 81 (2004): 1450–1456.

16. S. Neron, M. Morency, L. G. Chen, et al., "Diphenoquinones Redux," *Journal of Organic Chemistry* 87 (2022): 7673–7695.

17. (a) M. Kamali and Z. Pourghobadi, "Voltammetric Determination of Cysteine (2-Amino-3-Mercaptopropanoic Acid, CySH) by Means of 4,4'-Biphenol as a Homogeneous Mediator," *Iranian Journal of Pharmaceutical Research* 18 (2019): 1725–1734. (b) H. Shayani-Jam and D. Nematollahi, "Electrochemically Mediated Oxidation of Glutathione and N-Acetylcysteine With 4,4′-biphenol," *Electrochimica Acta* 56 (2011): 9311–9316.

18. M. Joudaki and D. Nematollahi, "A Green Electrochemical Method for the Synthesis of 2-(Phenylthio)-1 H -Benzo[d]Imidazole Derivatives," *Journal of the Electrochemical Society* 165 (2018): G133–G138.

19. K. Omura, "Rapid Conversion of Phenols to p-Benzoquinones Under Acidic Conditions With Lead Dioxide," *Synthesis* 1998 (1998): 1145–1148.

20. M. Yamada, K. Araki, and S. Shiraishi, "Oxygenation of 2,6-di-t-Butylphenol Catalysed by a New Cobalt(II) Complex [Co(babp)]: A Salen Analogue Having Higher Catalytic Activity, Selectivity, and Durability," *Journal of the Chemical Society, Perkin Transactions* 1 (1990): 2687–2690.

21. N. Scheiber, G. Blaser, E. M. Pferschy-Wenzig, M. Kaiser, P. Mäser, and A. Presser, "Efficient Oxidative Dearomatisations of Substituted Phenols Using Hypervalent Iodine (III) Reagents and Antiprotozoal Evaluation of the Resulting Cyclohexadienones Against *T. b. rhodesiense* and *P. falciparum* Strain NF54," *Molecules (Basel, Switzerland)* 27 (2022): 6559.

22. F. Sprang, J. D. Herszman, and S. R. Waldvogel, "Electrochemical Oxidation of Phenols in Flow: A Versatile and Scalable Access to Para -Benzoquinones," *Green Chemistry* 24 (2022): 5116–5124.

23. H. Nishino, N. Itoh, M. Nagashima, and K. Kurosawa, "Choice of Manganese(III) Complexes for the Synthesis of 4,4′-Biphenyldiols and 4,4′-Diphenoquiones," *Bulletin of the Chemical Society of Japan* 65 (1992): 620–622.

24. T. H. James, J. M. Snell, and A. Weissberger, "Oxidation Processes. XII. 1 the Autoxidation of Hydroquinone and of the Mono-, Di- and Trimethylhydroquinones," *Journal of the American Chemical Society* 60 (1938): 2084–2093.

25. M. Tsukayama, Y. Kawamura, T. Ishizuka, S. B. Hayashi, and F. Torii, "Improved, Rapid and Efficient Synthesis of Polymethoxyflavones Under Microwave Irradiation and Their Inhibitory Effects on Melanogenesis," *Heterocycles* 60 (2003): 2775–2784.

26. T. H. Coffield, A. H. Filbey, G. G. Ecke, and A. J. Kolka, "Some Reactions of 2,6-Dialkylphenols 1," *Journal of the American Chemical Society* 79 (1957): 5019–5023.

27. Z. Maeno, T. Mitsudome, T. Mizugaki, and K. Jitsukawa, "A Dual-Functional Heterogeneous Ruthenium Catalyst for the Green One-Pot Synthesis of Biphenols," *Catalysis Science & Technology* 7 (2017): 3205–3209.

28. S. Domagała, V. Steglińska, and J. Dziegieć, "Oxidative Kupplung Einiger 2, 6-Disubstituierter Phenolderivate in Perchlorsäure in Gegenwart von Cer (IV)-Ionen," *Chemical Monthly* 129 (1998): 761–768.

29. P. Hapiot and J. Pinson, "Multiple Reaction Pathways for the Oxidation of 2,6-Diphenylphenolates," *Journal of Electroanalytical Chemistry* 362 (1993): 257–265.

30. H. J. Wang and C. J. Yu, "Theoretical Study on Redox Potentials of Organic Radicals in Different Solvents," *Research on Chemical Intermediates* 36 (2010): 1003–1019.

31. (a) H. Svith, H. Jensen, J. Almstedt, et al., "On the Nature of Solvent Effects on Redox Properties," *Journal of Physical Chemistry A* 108 (2004): 4805–4811. (b) M. Jonsson, D. D. M. Wayner, and J. Lusztyk, "Redox and Acidity Properties of Alkyl-and Arylamine Radical Cations and the Corresponding Aminyl Radicals," *Journal of Physical Chemistry* 100 (1996): 17539–17543.

32. D. Bradley, G. Williams, and M. Lawton, "Drying of Organic Solvents: Quantitative Evaluation of the Efficiency of Several Desiccants," *Journal of Organic Chemistry* 75 (2010): 8351–8354.

33. S. Guha, T. Prabakar, and S. Sen, "Blue Light-Emitting Diode-Induced Direct C–H Functionalization of 1,4-Quinones With Aryl and Alkyl Boronic Acids," *Journal of Organic Chemistry* 87 (2022): 15421–15434.

34. S. Srivastava, A. Ali, A. Tyagi, and R. Gupta, "{Cu^{2+}–Co^{3+}–Cu^{2+}} and {Cu^{2+}–Fe^{3+}–Cu^{2+}} Heterobimetallic Complexes and Their Catalytic Properties," *European Journal of Inorganic Chemistry* 2014 (2014): 2113–2123.

35. A. Hamsath, J. D. Galloway, and R. D. J. S. Baxter, "Quinone C–H Alkylations via Oxidative Radical Processes," *Synthesis* 50 (2018): 2915–2923.

36. Y. Ohba, Y. Murakami, T. Sone, and H. Awano, "Synthesis of New Type Benzo[b]Thiophene Fused Quinones and Their Tetracyanoquinodimethane Derivatives," *Journal of Heterocyclic Chemistry* 34 (1997): 781–787.

37. A. Baschieri, R. Amorati, L. Valgimigli, and L. Sambri, "1-Methyl-1,4-Cyclohexadiene as a Traceless Reducing Agent for the Synthesis of Catechols and Hydroquinones," *Journal of Organic Chemistry* 84 (2019): 13655–13664.

38. J. Helfenbein, C. Lartigue, E. Noirault, et al., "Isotopic Effect Study of Propofol Deuteration on the Metabolism, Activity, and Toxicity of the Anesthetic," *Journal of Medicinal Chemistry* 45 (2002): 5806–5808.

39. H. Jia, M. He, S. Yang, X. Yu, and M. Bao, "Visible-Light-Driven Di-T -Butyl Peroxide-Promoted the Oxidative Homo- and Cross-Coupling of Phenols," *European Journal of Organic Chemistry* 2022 (2022): e202101469.

40. B. Dahms, P. J. Kohlpaintner, A. Wiebe, R. Breinbauer, D. Schollmeyer, and S. R. Waldvogel, "Selective Formation of 4,4′-Biphenols by Anodic Dehydrogenative Cross- and Homo-Coupling Reaction," *Chemistry: A European Journal* 25 (2019): 2713–2716.

41. L. Bering, M. Vogt, F. M. Paulussen, and A. P. Antonchick, "Selective, Catalytic, and Metal-Free Coupling of Electron-Rich Phenols and Anilides Using Molecular Oxygen as Terminal Oxidant," *Organic Letters* 20 (2018): 4077–4080.

Supporting Information

Additional supporting information can be found online in the Supporting Information section.